Proc. Natl. Acad. Sci. USA
Vol. 80, pp. 7183–7187, December 1983
Biophysics

Translational diffusion in phospholipid monolayers measured by fluorescence microphotolysis

(model membranes/monolayer–bilayer relationship/monolayer phase transition/photobleaching)

REINER PETERS AND KONRAD BECK

Max-Planck-Institut für Biophysik, Kennedy-Allee 70, 6000 Frankfurt 70, Federal Republic of Germany

Communicated by John J. Brauman, August 1, 1983

ABSTRACT **A method is described that eliminates surface flow in monolayers at the air–water interface and makes possible diffusion measurements by fluorescence microphotolysis ("photobleaching"). In contrast to previous studies that did not account for surface flow, lipid probe diffusion has been found to be similar in densely packed monolayers and in related bilayers. Furthermore, it seems that lipid diffusion is based on the same molecular mechanism in monolayers, bilayers, and potentially also cell membranes. In monolayers of L-α-dilauroylphosphatidylcholine (Lau_2-PtdCho) the translational diffusion coefficient *D* of the fluorescent lipid probe N-4-nitrobenzo-2-oxa-1,3 diazole egg phosphatidylethanolamine decreased from 110 $\mu m^2/s$ at a surface pressure $\Pi = 1$ mN/m to 15 $\mu m^2/s$ at $\Pi = 38$ mN/m ($T = 21$–22°C). Data could be fitted by the "free volume model." In monolayers of L-α-dipalmitoylphosphatidylcholine (Pam_2-PtdCho) *D* decreased by >3 orders of magnitude upon increasing Π at constant temperature, thus indicating a fluid-to-crystalline phase transition. In Lau_2-PtdCho/Pam_2-PtdCho monolayers phase separation has been visualized in the fluorescence microscope and the effect on *D* measured. These results suggest that monolayers are a promising model system for studying the molecular mobility of lipids and other cell membrane components.**

Molecular mobility in cell membranes has been studied by fluorescence microphotolysis ("photobleaching") (for review, see refs. 1–3) and various other techniques. Thus, the role of translational diffusion in electron transfer (4), receptor-mediated processes (5), and visual transduction (6) has been worked out in some detail. Frequently, however, the complex architecture of cell membranes makes it difficult to relate molecular mobility to function and suggests resort to simpler model systems. It has been recognized for many years (7) and emphasized recently (8) that monolayers spread at the air–water interface have large potentialities for studies of diffusion in two dimensions.

Previous studies of translational diffusion in monolayers spread at the air–water interface have yielded diffusion coefficients 1–2 orders of magnitude larger (9–11) than in bilayers (e.g., ref. 12). Furthermore, the well-known fluid-to-crystalline phase transition of phospholipid monolayers was reported (10) to have little effect on the diffusion coefficient. It appears that these discrepancies can now be understood on the basis of recent fluorescence microscopic observations (8): normally, monolayers at the air–water interface are subject to vigorous streaming probably induced by temperature fluctuations and bulk flow in both subphase and air. Surface streaming, of course, interferes with diffusion measurements and potentially can lead to gross overestimates of diffusion coefficients.

Therefore, we have developed a simple method (for an abstract, see ref. 13) for light-microscopic monolayer studies that minimizes surface streaming and renders possible diffusion measurements by fluorescence microphotolysis. The dependence on surface pressure (Π), fluid-to-crystalline phase transition, and fluid-crystalline phase separation of lipid probe diffusion in diacyl phosphatidylcholine monolayers has been measured. Results indicate that diffusion in monolayers is not so much different from that in bilayers as suggested previously. Rather, it appears that lipid diffusion in monolayers, bilayers, and membranes is based on the same molecular mechanism.

MATERIALS AND METHODS

Phospholipids. L-α-Dilauroylphosphatidylcholine (Lau_2-PtdCho) and L-α-dipalmitoylphosphatidylcholine (Pam_2-PtdCho) were obtained from Sigma and used without further purification. N-4-Nitrobenzo-2-oxa-1,3 diazole egg phosphatidylethanolamine (NBD-egg-PtdEtn) was from Avanti Polar Lipids, Birmingham, AL.

Monolayer Techniques. A small trough for microscopic studies (Fig. 1; details will be published elsewhere) was milled from polytetrafluoroethylene, with a surface of 70 cm^2. The surface balance was constructed according to Kuhn *et al.* (14). Its accuracy was about ±0.1 mN/m. The trough was thermostated and furthermore situated in a thermostated compartment built around the stage of the microscope. Experiments were initiated by an extensive cleaning of the trough. The trough was then filled to the brim with double-distilled water. The air–water interface was cleaned several times before spreading lipids from chloroform solutions (1 mM). Monolayers were allowed to stay at a $\Pi < 0.2$ mN/m for 10–30 min and then were slowly compressed to give Π increments of about 2.5 mN/m. After each compression, equilibration of Π was awaited before starting with diffusion measurements. Π-$\bar{a}$ isotherms were recorded by using a sensitive surface balance designed by Albrecht (15).

Multilamellar Vesicles. Large multilamellar vesicles with diameters of up to 100 μm were prepared as described (16).

Fluorescence Microphotolysis. The basic concepts of fluorescence microphotolysis (17), also quoted as fluorescence recovery after photobleaching (18) and fluorescence photobleaching recovery (19), have been described (17–22). The instrumental setup used in this study was essentially as described by Peters and Richter (23). The 488-nm line of an argon laser was used and focused to a spot of gaussian intensity profile with an e^{-2} radius of 18 μm (×16 objective lens). Fluorescence was measured by single-photon counting equipment and data were processed by a microcomputer (DEC MINC 11/23). Data were in most cases evaluated according to equation 19 of Axelrod *et al.*

The publication costs of this article were defrayed in part by page charge payment. This article must therefore be hereby marked "*advertisement*" in accordance with 18 U.S.C. §1734 solely to indicate this fact.

Abbreviations: NBD-egg-PtdEtn, N-4-nitrobenzo-2-oxa-1,3 diazole egg phosphatidylethanolamine; Lau_2-PtdCho, L-α-dilauroylphosphatidylcholine; Pam_2-PtdCho, L-α-dipalmitoylphosphatidylcholine; *D*, translational diffusion coefficient; Π, surface pressure.

(19). Selected data were analyzed according to Yguerabide *et al.* (24).

Microphotography. Photographs, taken on Kodak Tri-X film and developed with Emofin (Tetanal, Hamburg, FRG) to 3,200 ASA, required usually 8 s of exposure time.

RESULTS

The Monolayer Technique. Our method is based on the observation that vigorous streaming normally observed in monolayers at the air–water interface can be eliminated by isolating a small area of the monolayer from that remaining. A schematic drawing of the setup is given in Fig. 1. A small trough that fits on the stage of a fluorescence microscope has been milled from a piece of polytetrafluoroethylene. A surface balance of the Whilhemy type and a barrier provide for control of Π and mean molecular area $\bar{a}$. The essential new feature simply consists of a 2-mm-thick plate that is placed across the trough at one end. The plate contains holes of 3–5 mm in diameter for microscopic and Π measurements, respectively. Holes and free surface are connected by canals, which, in the present study, were 2 mm wide. However, canal width can be made larger if required by monolayer viscosity. Experiments are initiated by filling the trough to the brim with a suitable subphase, which was pure water in experiments reported here. The monolayer-forming substance is spread at the free air–water interface and compressed as desired. Absence of surface streaming has been checked by an analysis of the fluorescence recovery curves according to Yguerabide *et al.* (24), by direct fluorescence microscopic observations, and by microphotography. Micrographs of inhomogeneously fluorescent monolayers as shown in Figs. 3 and 4 possibly provided the most sensitive indicator for absence of flow because sharp images have been obtained even if exposure times were much larger than diffusion times (i.e., half-time of fluorescence recovery).

Translational Diffusion in Lau_2-PtdCho Monolayers. Lau_2-PtdCho monolayers, at 21–22°C, are in a fluid phase throughout the range of Π applied in this study—i.e., 1–38 mN/m. Our measurements concerned monolayers of Lau_2-PtdCho and NBD-egg-PtdEtn mixed at a molar ratio of 100:1. This probe concentration did not have any effect on monolayer properties, as judged from Π-$\bar{a}$ isotherms (not shown). Results of diffusion measurements are displayed in Fig. 2. According to the "free volume model" of translational diffusion (26–28), which will be discussed below, data have been plotted as ln D vs. $1/a_f$, in which a_f is the free molecular area; a_f is defined as $\bar{a}$ minus minimum molecular area a_0. The direct experimental variable Π and $\bar{a}$ as derived from Π-$\bar{a}$ diagrams are also given. D decreased monotonously from 110 $\mu m^2/s$ at Π = 1 mN/m to 15 $\mu m^2/s$ at 38 mN/m. After photobleaching, fluorescence recovered to 100% in all cases, indicating absence of immobile fractions. Fluorescence microscopic observations showed monolayer fluorescence to be completely homogeneous throughout the Π range studied.

Translational Diffusion in Lau_2-PtdCho Bilayers. To provide a direct comparison of monolayers and bilayers, diffusion in large multilamellar vesicles has been measured. By using the same instrumental parameters and Lau_2-PtdCho/NBD-egg-PtdEtn mixtures as in the monolayer studies, D has been determined to be 7.7 ± 1.0 $\mu m^2/s$ (mean ± SD of 15 measurements; T = 21–22°C).

Translational Diffusion in Pam_2-PtdCho Monolayers. In contrast to Lau_2-PtdCho monolayers, Pam_2-PtdCho monolayers are known to undergo a phase transition upon raising Π at constant temperature. This isothermal fluid-to-crystalline transition has been studied by surface balance techniques (25, 29, 30). The transition is apparent as a shoulder of the Π-$\bar{a}$ isotherm, which, according to our measurements on Pam_2-PtdCho/NBD-egg-PtdEtn (100:1, mol/mol) monolayers, extends from 4 to 14 mN/m at 21–22°C. In the following, we quote this Π range as the "intermediate region." Results are given in Fig. 3. D decreased to <1/1,000 with increasing Π. The steepest decline of D has been observed between 8 and 10 mN/m, in which Π range D dropped from >10 $\mu m^2/s$ to <0.2 $\mu m^2/s$. After photobleaching, fluorescence recovered to 100% in all cases of $\Pi \leqq 9$ mN/m. In contrast to Lau_2-PtdCho monolayers, the fluorescence of Pam_2-PtdCho monolayers was not homogeneous throughout the whole Π range (Fig. 3 *Insets*): in the

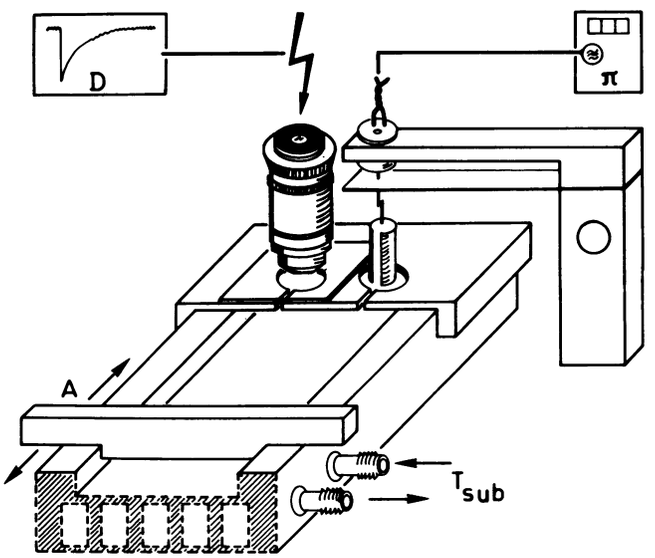

FIG. 1. A trough for measurement of translational diffusion in monolayers spread at the air–water interface (not drawn to scale). To prevent surface flow, a 2-mm-thick plate is placed across the air–water interface at one end of the trough. The plate contains holes (diameter, 3–5 mm) for microscopic and surface balance measurements, respectively. Holes and free surface are connected by 2-mm-wide canals. Translational diffusion has been measured by fluorescence microphotolysis (photobleaching).

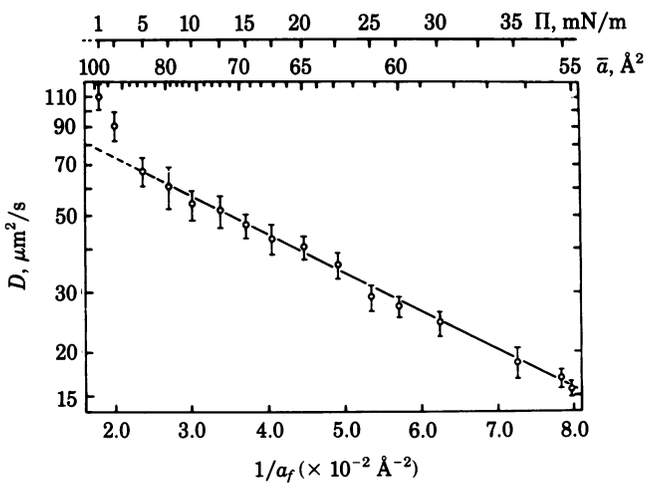

FIG. 2. Lipid probe diffusion in Lau_2-PtdCho monolayers. The translational diffusion coefficient (D) of the fluorescently labeled phospholipid NBD-egg-PtdEtn has been measured in Lau_2-PtdCho monolayers (T = 21–22°C). Values are mean ± SD of about 10 measurements using 3 monolayers. Data are plotted according to the free volume model (see text) as ln D vs. $1/a_f$, in which a_f is the free area per molecule. Scales of Π and mean molecular area $\bar{a}$ are also given.

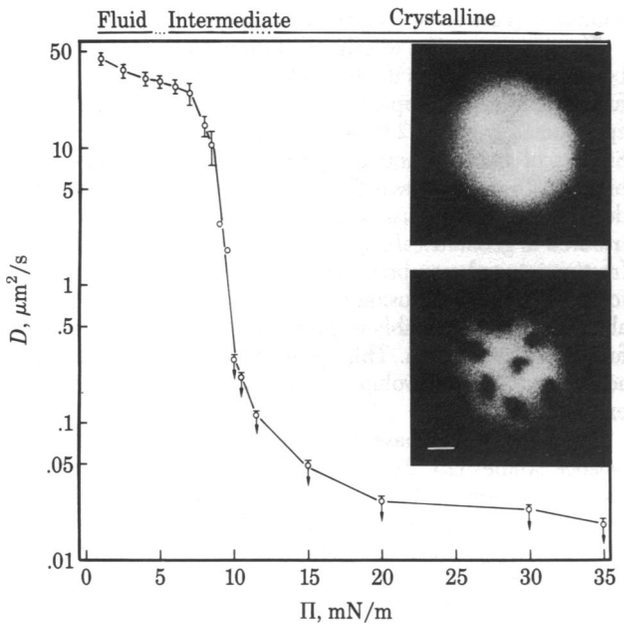

FIG. 3. The fluid-to-crystalline phase transition in Pam_2-PtdCho monolayers. The D of the fluorescently labeled phospholipid NBD-egg-PtdEtn in Pam_2-PtdCho monolayers has been measured as a function of Π (T = 21–22°C). Values are mean ± SD of about 10 measurements using 3 monolayers. Arrows indicate that D values are upper limits. Monolayer phases and corresponding Π ranges are indicated at the top. (*Insets*) Typical monolayer fluorescence at 2.5 mN/m (upper) and 7.0 mN/m (lower), respectively (bar = 10 μm). In the crystalline phase (Π ≧ 14 mN/m) monolayer fluorescence was as homogeneous (micrograph not shown) as in the fluid phase. In the micrographs the irradiated area is the same one employed in diffusion measurements (gaussian intensity profile, e^{-2} radius = 18 μm).

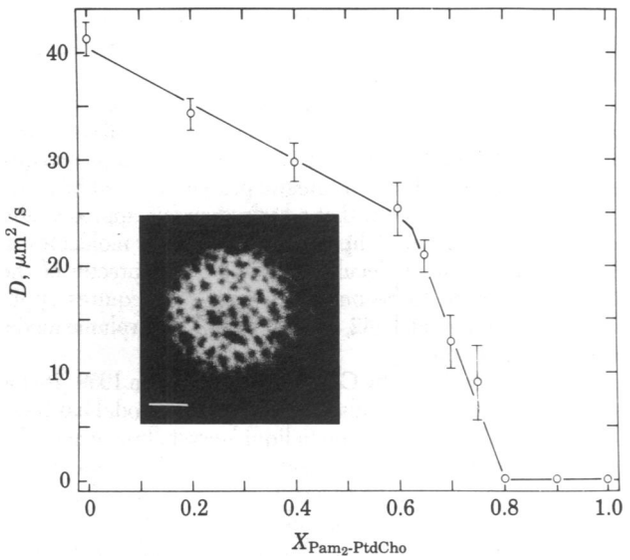

FIG. 4. Phase separation in mixed monolayers. The D of the fluorescently labeled phospholipid NBD-egg-PtdEtn in monolayers of Lau_2-PtdCho/Pam_2-PtdCho mixtures is given as a function of monolayer composition. Values are mean ± SD of about 10 measurements; Π = 20 mN/m; T = 21–22°C. (*Inset*) Typical monolayer fluorescence at a mol fraction of Pam_2-PtdCho $X_{Pam_2\text{-}PtdCho}$ = 0.70 (bar = 10 μm). For $X_{Pam_2\text{-}PtdCho} < 0.5$, monolayer fluorescence was homogeneous (not shown).

intermediate region, nonfluorescent patches were visible, which first appeared at ≈4 mN/m, became larger with increasing Π, and gradually vanished again at ≈14 mN/m.

Translational Diffusion in Monolayers Prepared from Lau_2-PtdCho/Pam_2-PtdCho Mixtures. Both fluorescence inhomogeneity and the steep decline of D suggest the intermediate region of Pam_2-PtdCho monolayers to be a state of coexisting fluid and crystalline domains. To substantiate this hypothesis, we have studied a monolayer system in which phase separation was to be anticipated—namely, monolayers of Lau_2-PtdCho/Pam_2-PtdCho mixtures. Lau_2-PtdCho and Pam_2-PtdCho differ in chain length by four CH_2 groups. In bilayers, depending of course on parameters such as molar ratio, temperature, ionic strength, etc., such a difference in chain length leads to separation of crystalline and fluid domains (31). In monolayers of Lau_2-PtdCho/Pam_2-PtdCho mixtures to which NBD-egg-PtdEtn had been added to a final molar fraction of 0.01, evidence for phase separation has been obtained by surface balance measurements (not shown). At 21–22°C Π-$\bar{a}$ isotherms were smooth for monolayers in which the mol fraction of Pam_2-PtdCho $X_{Pam_2\text{-}PtdCho}$ was <0.5. At $X_{Pam_2\text{-}PtdCho}$ = 0.5, first indications of a shoulder appeared, which became increasingly prominent with increasing $X_{Pam_2\text{-}PtdCho}$.

A micrograph and diffusion measurements are given in Fig. 4 for the case in which Π had been adjusted to a constant value of 20 mN/m. At $X_{Pam_2\text{-}PtdCho} < 0.5$, monolayer fluorescence was completely homogeneous and diffusion coefficients decreased only moderately with $X_{Pam_2\text{-}PtdCho}$. At $X_{Pam_2\text{-}PtdCho}$ = 0.5, nonfluorescent patches appeared, which were similar to those observed in the intermediate region of Pam_2-PtdCho monolayers. The area fraction of nonfluorescent patches increased with $X_{Pam_2\text{-}PtdCho}$. A rather steep decline of D occurred between $0.6 \leqq X_{Pam_2\text{-}PtdCho} \leqq 0.8$. After photobleaching, fluorescence recovered to 100% in all cases of $X_{Pam_2\text{-}PtdCho} \leqq 0.8$.

DISCUSSION

Similarities and differences between monolayers and bilayers have been the subject of a long-standing discussion (25, 29, 30, 32–35). Argumentation was mainly based on surface balance measurements and thermodynamic considerations. The main objective of this communication is to provide direct experimental evidence revealing new analogies of monolayers and bilayers: in both systems, the lipid probe diffusion coefficient is similar at comparable molecular density, diffusion apparently is based on the same molecular mechanism, and the fluid-to-crystalline phase transition of the monolayer is accompanied by a >1,000-fold reduction of diffusion coefficient as is the liquid–liquid crystalline transition of the bilayer. In the following, some of these aspects will be discussed in detail and on a more quantitative level.

Simultaneously with us, v. Tscharner and McConnell (8) have observed that monolayers at the air–water interface can be subject to vigorous streaming. In Pam_2-PtdCho monolayers this streaming was found to be rapid at large and slow at small mean molecular area $\bar{a}$. Transfer of the monolayer onto alkylated glass slides (36–38) abolished streaming, while lipid probe mobility—to a certain extent—was retained. Thus, in transferred monolayers the lipid probe diffusion coefficient has been determined to be about 1 $\mu m^2/s$ for all values of $\bar{a}$ equal to or larger than 45 $Å^2$. Fluorescence inhomogeneities very similar to those reported in this study have been also observed in NBD-egg-PtdEtn-doped Pam_2-PtdCho monolayers on solid substrates (R. Weis and H. M. McConnell, personal communication).

The Molecular Mechanism of Translational Diffusion in Monolayers, Bilayers, and Cell Membranes. The mobility of proteins in cell membranes and reconstituted bilayers has been

frequently discussed with respect to the hydrodynamic theory of Saffman and Delbrück (39–41). We have recently provided an experimental test of the Saffman–Delbrück equations by measuring both translational and rotational diffusion of bacteriorhodopsin in dimyristoylphosphatidylcholine bilayers (16), which suggests that the Saffman–Delbrück equations correctly describe diffusive mobility of integral proteins in fluid bilayers. However, it is not evident that a hydrodynamic approach also holds for the diffusion of lipids and other small molecules in bilayers. Rather, the molecular discontinuous character of the bilayer is expected to become effective. This requires application of different models (42, 43), such as the free volume model to be discussed now.

Originally introduced by Cohen and Turnbull in 1959 (26) for molecular transport in liquids, the free volume model has been adopted to lipid probe diffusion in liquid–crystalline bilayers by Sackmann, Träuble, and colleagues (27, 28). Lipid molecules are modeled by hard rods of cross section a_0 moving in the membrane plane with a local velocity u. Most of the time, movement is confined to a cage bounded by immediate neighbors. Density fluctuation occasionally opens up a hole that is large enough to allow for a displacement of the trapped molecule. On these grounds, the following expression for the D has been derived:

$$D = g\, d\, u \exp(-\gamma\, a^*/a_f), \qquad [1]$$

in which g is a geometric factor close to unity, d approximately equals the molecular diameter, a_f is the free area as defined ($a_f = \bar{a} - a_0$), a^* is the critical free area at which a displacement becomes possible, and γ is a factor accounting for overlap of free area ($0.5 < \gamma < 1.0$).

We have applied the free volume model to lipid probe diffusion in fluid monolayers. This was particularly interesting because free area can be varied over a large range in the case of monolayers. Eq. 1 may be rearranged to give a linear relationship:

$$\ln D = A - B/a_f, \qquad [2]$$

in which $A = g\, d\, u$ and $B = \gamma\, a^*$. Plotting the data of Lau_2-PtdCho monolayers as ln D vs. $1/a_f$ (Fig. 2) yields a straight line as predicted by Eq. 2. Linearity has been optimized by systematically varying a_0. The correlation coefficient of linear regression had a maximum value of 0.9973 at $a_0 = 42.5$ Å^2, a molecular area that is in excellent agreement with structural data of crystalline mono- and bilayers (44). In Fig. 2 a significant deviation from linearity is only observed at large a_f ($a_f > 2\, a_0$). Leaving this a_f range out of consideration, an evaluation of coefficients A and B yields 124 μm^2/s as a limiting upper value of D ($1/a_f \rightarrow 0$) and 26.0 Å^2 for γa^*—i.e., 26 Å^2 $< a^* <$ 52 Å^2. These results clearly speak for the applicability of the free volume model to lipid probe diffusion in monolayers and therefore also suggest that lipid diffusion is based on the same molecular mechanism in monolayers and bilayers.

Absolute D values are somewhat smaller in bilayers than monolayers—e.g., $D = 7.7$ μm^2/s for Lau_2-PtdCho bilayers and 15 μm^2/s for Lau_2-PtdCho monolayers at $\Pi = 38$ mN/m. Evidence obtained by fluorescence anisotropy decay measurements (45) and x-ray (46) and neutron diffraction (47) suggests a substantial degree of interdigitation of hydrocarbon chains at the bilayer midplane. Rotational isomerization of the hydrocarbon chains and the formation of "kinks" presumably is the basic mechanism of creating free volume in bilayers. Once formed in a segment of a chain, a kink can be easily propagated along the same chain. It is conceivable that interdigitation hinders propagation of kinks and that in this manner effective free volume is reduced in bilayers as compared to monolayers.

The question arises whether diffusion in cell membranes can be also understood on the basis of the free volume model. Diffusion coefficients of lipid probes in cell membranes range from approximately 0.2 to 2.0 μm^2/s (see, e.g., ref. 1 for review). Studies of bacteriorhodopsin/dimyristoylphosphatidylcholine bilayers (16) have shown that integral membrane proteins reduce lipid probe diffusion. Much of this reduction can be attributed to geometrical parameters: at high weight and volume fraction integral membrane proteins form a geometric obstacle to the long-range diffusion of lipids. More important than the absolute D value possibly is the insensitivity of lipid probe diffusion to chain length. This speaks for a diffusion mechanism according to the free volume model but certainly needs further experimental testing.

The Monolayer Phase Transition. On the basis of surface balance studies (25, 29, 30) parallels between the isothermal phase transition of the monolayer and the liquid crystalline–crystalline phase transition of bilayers have been drawn. However, a matter of much discussion was the circumstance that the Π-$\bar{a}$ isotherm in the intermediate region between fluid and crystalline monolayer phase is not completely horizontal—i.e., Π is not constant. In a strict sense, this fact appeared to be inconsistent with a first-order transition mechanism and thus seemed to devaluate a direct comparison of phase transitions in monolayers and bilayers. However, Albrecht *et al.* (30) have proposed that a finite slope of the Π-$\bar{a}$ isotherm would be compatible with a first-order transition mechanism if cooperativity were restricted to units of limited size. If so, a Pam_2-PtdCho monolayer in the intermediate region should be made up of coexisting fluid and solid domains. We have indeed observed (Fig. 3 *Insets*) that monolayer fluorescence is inhomogeneous between 4 and 14 mN/m. We assume that nonfluorescent patches are crystalline domains and that the probe NBD-egg-PtdEtn, if it has a choice, partitions almost exclusively in the fluid phase (see ref. 48 for discussion of phase partition preference of fluorescent lipid probes). Support for this interpretation is provided by the studies of phase separation in Lau_2-PtdCho/Pam_2-PtdCho monolayers. With the onset of phase separation at $X_{Pam_2\text{-PtdCho}} = 0.5$ ($\Pi = 20$ mN/m), fluorescence became inhomogeneous and D decreased in a fashion (Fig. 4) very similar to that in the intermediate region of Pam_2-PtdCho monolayers.

The isothermal monolayer phase transition is accompanied by a reduction to <1/1,000 of lipid probe diffusion (Fig. 3). This is very similar to the reduction of lipid probe diffusion in phospholipid bilayers by the liquid crystalline–crystalline main phase transition (for review, see ref. 12). This confirms the conclusion that previously had been drawn mainly from indirect evidence such as Π-$\bar{a}$ isotherms—namely, that Pam_2-PtdCho monolayers undergo a transition from a fluid to a crystalline phase. In the monolayer case the largest decrease of D occurs over a narrow Π range (8–10 mN/m), whereas the phase transition region extends from 4 to 14 mN/m. From statistical calculations (49) simulating the effect on diffusion of impermeable clusters dispersed in a fluid membrane, such behavior can indeed be expected. The reduction of lipid probe diffusion can be understood as a percolation phenomenon (for review, see also ref. 50): depending on the area fraction of solid clusters, long-range diffusion in the fluid phase will be reduced and eventually, at the percolation threshold, will be completely blocked. Lau_2-PtdCho/Pam_2-PtdCho monolayers, again, showed an analogous behavior. The steep decrease of D was observed around $X_{Pam_2\text{-PtdCho}} = 0.70$, right in the middle of phase separation region.

Thus, diffusion measurements and fluorescence microscopic

observations support the contention that Pam_2-PtdCho monolayers undergo a fluid-to-crystalline phase transition passing through a region in which fluid and solid domains coexist. According to Albrecht *et al.* (30), this fact can explain why the Π-$\bar{a}$ isotherm is not completely horizontal in the intermediate region. However, cooperative units, as calculated by Albrecht *et al.* (30) from the slope of Π-$\bar{a}$ isotherms, comprise $\approx 10^2$ molecules, whereas nonfluorescent patches seen in the microscope are made up of $\approx 10^6$ molecules. These patches may be aggregates of the primary cooperative units because solid domains, as long as they are small, will retain a high diffusional mobility and will aggregate quickly.

CONCLUSION

Monolayers as a Model System for Studying Molecular Mobility of Cell Membrane Components. Monolayers have been frequently used to study lipid–protein interaction and refined techniques have been developed for that purpose (e.g., see ref. 51). In many cases, of course, protein denaturation at interfaces sets a limit to meaningful experiments. However, the production of bilayer membranes from monolayer precursors (52) suggests that at least a number of important integral membrane proteins can pass through a monolayer state in functional form. Regardless of the question of whether it is wise to employ monolayers for protein studies, monolayers certainly are an excellent system for basic studies of lipid diffusion in two dimensions. Easy control of molecular density is an outstanding feature of monolayers and we have shown how this can be exploited to study the molecular basis of translational diffusion and phase transition.

We thank Dr. O. Albrecht for permission to use his surface balance. Support by the Deutsche Forschungsgemeinschaft is gratefully acknowledged.

1. Peters, R. (1981) *Cell Biol. Int. Rep.* **5**, 733–760.
2. Cherry, R. J. (1979) *Biochim. Biophys. Acta* **559**, 289–327.
3. Edidin, M. (1981) in *Membrane Structure*, eds. Finean, J. B. & Michell, R. H. (Elsevier/North-Holland, New York), pp. 39–82.
4. Hackenbrock, C. R. (1981) *Trends Biochem. Sci.* **6**, 151–154.
5. Pastan, I. H. & Willingham, M. C. (1981) *Science* **214**, 504–509.
6. Liebman, P. A. & Pugh, E. N., Jr. (1979) *Vision Res.* **19**, 375–380.
7. Shah, D. O. (1972) in *Progress in Surface Science*, ed. Davison, S. G. (Pergamon, Oxford), Vol. 3, Part 3, pp. 221–278.
8. v. Tscharner, V. & McConnell, H. M. (1981) *Biophys. J.* **36**, 409–419.
9. Stroeve, P. & Miller, J. (1975) *Biochim. Biophys. Acta* **401**, 157–167.
10. Teissie, J., Tocanne, J. F. & Baudras, A. (1978) *Eur. J. Biochem.* **83**, 77–85.
11. Loughran, T., Hatlee, M. D., Patterson, L. K. & Kozak, J. J. (1980) *J. Chem. Phys.* **72**, 5791–5797.
12. Vaz, W. L. C., Derzko, Z. I. & Jacobson, K. A. (1982) in *Membrane Reconstitution*, eds. Poste, G. & Nicolson, G. L. (Elsevier Biomedical, Amsterdam), pp. 83–136.
13. Beck, K. & Peters, R. (1982) *Hoppe-Seyler's Z. Physiol. Chem.* **363**, 894 (abstr.).
14. Kuhn, H., Möbius, D. & Bücher, H. (1972) in *Physical Methods of Chemistry*, eds. Weissberger, A. & Rossiter, B. (Wiley, New York), Vol. 1, Part 3B, pp. 651–653.
15. Albrecht, O. (1983) *Thin Solid Films* **99**, 227–234.
16. Peters, R. & Cherry, R. J. (1982) *Proc. Natl. Acad. Sci. USA* **79**, 4317–4321.
17. Peters, R., Peters, J., Tews, K. H. & Bähr, W. (1974) *Biochim. Biophys. Acta* **367**, 282–294.
18. Jacobson, K., Wu, E.-S. & Poste, G. (1976) *Biochim. Biophys. Acta* **433**, 215–222.
19. Axelrod, D., Koppel, D. E., Schlessinger, J., Elson, E. & Webb, W. W. (1976) *Biophys. J.* **16**, 1055–1069.
20. Edidin, M., Zagyanski, Y. & Larner, T. J. (1976) *Science* **191**, 466–468.
21. Smith, B. A. & McConnell, H. M. (1978) *Proc. Natl. Acad. Sci. USA* **75**, 2759–2763.
22. Peters, R., Brünger, A. & Schulten, K. (1981) *Proc. Natl. Acad. Sci. USA* **78**, 962–966.
23. Peters, R. & Richter, H.-P. (1981) *Dev. Biol.* **86**, 285–293.
24. Yguerabide, J., Schmidt, J. A. & Yguerabide, E. E. (1982) *Biophys. J.* **39**, 69–75.
25. Phillips, M. C. & Chapman, D. (1968) *Biochim. Biophys. Acta* **163**, 301–313.
26. Cohen, M. H. & Turnbull, D. (1959) *J. Chem. Phys.* **31**, 1164–1169.
27. Träuble, H. & Sackmann, E. (1972) *J. Am. Chem. Soc.* **94**, 4499–4510.
28. Galla, H. J., Hartmann, W., Theilen, U. & Sackmann, E. (1979) *J. Membr. Biol.* **48**, 215–236.
29. Nagle, J. F. (1976) *J. Membr. Biol.* **27**, 233–250.
30. Albrecht, O., Gruler, H. & Sackmann, E. (1978) *J. Phys. (Paris)* **39**, 301–313.
31. Shimshick, E. J. & McConnell, H. M. (1973) *Biochemistry* **12**, 2351–2360.
32. Gershfeld, N. L. (1976) *Annu. Rev. Phys. Chem.* **27**, 349–368.
33. Cadenhead, D. A., Müller-Landau, F. & Kellner, B. M. J. (1980) in *Ordering in Two Dimensions*, ed. Sinha, S. K. (Elsevier Biomedical Press, Amsterdam), pp. 73–81.
34. Nagle, J. F. (1980) *Annu. Rev. Phys. Chem.* **31**, 157–195.
35. Lis, L. J., McAllister, M., Fuller, N. & Rand, R. P. (1982) *Biophys. J.* **37**, 667–672.
36. v. Tscharner, V. & McConnell, H. M. (1981) *Biophys. J.* **36**, 421–427.
37. Hafeman, D. G., v. Tscharner, V. & McConnell, H. M. (1981) *Proc. Natl. Acad. Sci. USA* **78**, 4552–4556.
38. Weis, R. M., Balakrishnan, K., Smith, B. A. & McConnell, H. M. (1982) *J. Biol. Chem.* **257**, 6440–6445.
39. Saffman, P. G. & Delbrück, M. (1975) *Proc. Natl. Acad. Sci. USA* **72**, 3111–3113.
40. Saffman, P. G. (1976) *J. Fluid Mech.* **73**, 563–602.
41. Hughes, B. D., Pailthorpe, B. A. & White, L. R. (1982) *J. Fluid Mech.* **110**, 349–372.
42. Vaz, W. L. C., Criado, M., Madeira, V. M. C., Schoellmann, G. & Jovin, Th. M. (1982) *Biochemistry* **21**, 5608–5612.
43. Vaz, W. L. C. & Hallmann, D. (1983) *FEBS Lett.* **152**, 287–290.
44. Hui, S. W., Cowden, M., Papahadjopoulos, D. & Parsons, D. F. (1975) *Biochim. Biophys. Acta* **382**, 265–275.
45. Vincent, M., de Foresta, B., Galley, J. & Alfsen, A. (1982) *Biochemistry* **21**, 708–716.
46. Cain, J., Santillan, G. & Blaisie, J. K. (1972) in *Membrane Research*, ed. Fox, C. F. (Academic, New York), pp. 3–14.
47. Zaccai, G., Büldt, G., Seelig, A. & Seelig, J. (1979) *J. Mol. Biol.* **134**, 693–706.
48. Klausner, R. D. & Wolf, D. E. (1980) *Biochemistry* **19**, 6199–6203.
49. Freire, E. & Snyder, B. (1982) *Biophys. J.* **37**, 617–624.
50. Saxton, M. J. (1982) *Biophys. J.* **39**, 165–173.
51. Fromherz, P. (1971) *Biochim. Biophys. Acta* **225**, 382–386.
52. Montal, M., Darszon, A. & Schindler, H. (1981) *Q. Rev. Biophys.* **14**, 1–79.